# PHILOSOPHICAL TRANSACTIONS A

royalsocietypublishing.org/journal/rsta





Article submitted to journal

#### **Subject Areas:**

warm dense matter, ion transport properties, molecular dynamics

#### Keywords:

xxxx, xxxx, xxxx

#### Author for correspondence:

Thomas G. White e-mail: tgwhite@unr.edu

# Disentangling the Effects of Non-Adiabatic Interactions upon Ion Self-Diffusion within Warm Dense Hydrogen

William A. Angermeier<sup>1</sup>, Brett S. Scheiner<sup>2</sup>, Nathaniel R. Shaffer<sup>3</sup>, Thomas G. White<sup>1</sup>

Warm dense matter is a material state in the region of parameter space connecting condensed matter to classical plasma physics. In this intermediate regime, we investigate the significance of nonadiabatic electron-ion interactions upon ion dynamics. To disentangle non-adiabatic from adiabatic electronion interactions, we compare the ion self-diffusion coefficient from the non-adiabatic electron force field computational model to an adiabatic, classical molecular dynamics simulation. A classical pair potential developed through a force-matching algorithm ensures the only difference between the models is due to the electronic inertia. We implement this new method to characterize non-adiabatic effects on the self-diffusion of warm dense hydrogen over a wide range of temperatures and densities. Ultimately we show that the impact of non-adiabatic effects is negligible for equilibrium ion dynamics in warm dense hydrogen.

<sup>&</sup>lt;sup>1</sup>Department of Physics, University of Nevada, Reno NV 89557, USA

<sup>&</sup>lt;sup>2</sup>Los Alamos National Laboratory, Los Alamos, New Mexico 87545, USA

<sup>&</sup>lt;sup>3</sup>Laboratory for Laser Energetics, University of Rochester, Rochester, New York 14623, USA

### 1. Introduction

Warm dense matter (WDM) is an intermediate state of matter that approximately spans a density range of 0.01-100 g/cm³ and temperatures from 0.1-100 eV [1,2]. Simulations of WDM typically employ the Born-Oppenheimer (BO) approximation, also known as the adiabatic approximation, which dictates that the electrons adjust instantaneously to the ion fields [3]. Usually justified through the disparate energy scales of the electron and ion motion, it is the cornerstone of modern simulation techniques in both physics and chemistry [4,5]. Whether such a fundamental premise holds in the extreme states of matter in the center of planets and stars is ultimately unknown. Recent attempts to remove this approximation have led to conflicting predictions of the sensitivity of ion dynamics to non-adiabatic effects. Given the lack of theoretical consensus and the dearth of experimental data on ion transport properties in the WDM regime, the importance of non-adiabatic effects is still under scrutiny [6–11].

Non-adiabatic effects are ordinarily associated with non-equilibrium processes in which significant energy exchange occurs between the plasma components. The classic example in WDM is temperature equilibration between electrons and ions [12,13]. Many authors have claimed that non-adiabatic effects can also influence processes in equilibrium, such as ion self-diffusion [10] and ion acoustic wave propagation [7,8]. However, these claims are difficult to test using available simulation methods, where it is complicated to disentangle the effects of non-adiabatic interactions from the approximations used for treating the electrons. The primary focus of this paper is to unambiguously determine whether non-adiabatic effects (i.e., those that do not employ the BO approximation) are relevant to ion self-diffusion in equilibrium WDM. Ion self-diffusion was chosen as the ion transport property of interest as it is simple to obtain computationally and was recently predicted to have a large sensitivity to non-adiabatic effects [10].

**Table 1.** Ion self-diffusion coefficient of warm dense hydrogen from DFT and eFF simulations for four specific densities and temperatures.  $\Gamma=(Ze)^2/ak_BT$  is the coulomb coupling parameter, where  $a=(3/4\pi n)^{1/3}$  is the Wigner-Seitz radius, n is the ion number density, T is the temperature, and Z is the average ion charge state which estimated using the Thomas-Fermi model [11,14].  $\Theta=k_BT/E_F$  is the electron degeneracy parameter, where  $E_F=\hbar^2(3\pi^2Zn)^{2/3}/2m_e$  is the Fermi energy [15].

$\rho  (g/cm^3)$	T (eV)	Z	Γ	Θ	$D_{ m DFT}~({ m cm}^2/{ m s})$	$D_{\rm eFF}~({\rm cm}^2/{\rm s})$
0.7	1.5	0.66	5.06	0.10	0.016	0.009
0.7	4.5	0.67	1.74	0.29	0.053	0.024
5.0	25.0	0.82	0.90	0.38	0.083	0.059
21.73	20.0	0.88	2.09	0.11	0.020	0.019

The ideal approach to quantifying non-adiabatic effects on ion dynamics would be to compare adiabatic density functional theory molecular dynamics (DFT-MD) simulation results to a similarly high-fidelity non-adiabatic method, such as time-dependent DFT-MD. Unfortunately, the high computational cost of such methods makes them infeasible to study the ion dynamics in WDM. This high computational cost has led to the development of faster non-adiabatic simulation methods, such as the electron force field method (eFF), but these faster methods rely on many simplifying approximations to speed up calculations [7,16–18].

One would like to attribute discrepancies between DFT and eFF predictions to non-adiabatic effects, but the approximations used for treating the electrons in eFF are so simplified [18,19] compared to DFT that such a comparison is dubious [9,10]. Table 1 shows the ion self-diffusion coefficient for various temperatures and densities across the WDM regime using DFT-MD and eFF. The DFT-MD data was obtained using the Kohn-Sham DFT (KS-DFT) formulation, with the simulation details outlined in the supplemental material. Noticeable differences are seen between

the DFT and eFF at some conditions, but we cannot conclusively ascribe non-adiabatic effects as the primary explanation. To avoid equating models with fundamentally different theoretical underpinnings, we have developed a method based on the electron force field (eFF) technique that allows for direct examination of non-adiabatic effects while controlling for the approximations made by the underlying model.

To investigate the relevance of non-adiabatic effects on the ion dynamics in WDM, we compare the ion self-diffusion coefficients calculated from a non-adiabatic and adiabatic simulation. However, in contrast to previous work [10], we utilize a force-matching technique to extract an effective ion-ion interaction potential from the non-adiabatic simulation for use in a classical adiabatic MD simulation. We can then compare the ion self-diffusion predicted from each simulation approach to isolate non-adiabatic effects on the ion dynamics. Since both approaches are derived from eFF, the comparison is fair and avoids the problems inherent in comparing eFF with DFT.

# 2. Method

We use eFF as our non-adiabatic simulation method [6,19] and Potfit as our force-matching code [20-22]. eFF is a flavor of the wave packet molecular dynamics method that treats the electrons as quantum mechanical entities while the ions remain classical point-like particles; both the electrons and ions are simultaneously propagated forward in time according to Hamilton's equations of motion. The wave packet molecular dynamics methodology intrinsically incorporates non-adiabatic effects by allowing the electrons and ions to move together. In eFF, several significant simplifications allow the electrons to evolve in time with classical equations of motion while retaining a quantum mechanical description. These include using a single spherical Gaussian to describe each electron's wave packet, treating electrons as distinguishable particles using a Hartree product for the total wave function, and adding empirically parameterized Pauli potentials to account for the neglect of anti-symmetry [6,18]. Despite the uncontrolled approximations in eFF, no high-fidelity alternative exists for simulating non-adiabatic dynamics over the long timescales needed to compute ion transport properties. Improvements to the current eFF model that would provide a more robust alternative would be to increase the basis for each electron wave packet, implement a better approximation to the exchange energy, and incorporate a direct approximation for the electron correlation energy. All of these additions have been studied in a previous publication [18].

In addition, eFF allows for the dynamic electron mass,  $M_e$ , to be altered, which has previously been utilized to increase the simulation time step to provide a reduced computational wall time [6]. However, variation of the dynamic electron mass has also been used to modify non-adiabatic electron-ion interactions to allow eFF simulations to better match experimental data [23–26]. In adiabatic simulations such as DFT-MD, the electrons' mass can be thought of as effectively zero, which allows them to respond instantaneously to the motion of the ions in the simulation. Thus, as the dynamic electron mass approaches zero, eFF simulations satisfy the BO approximation and become adiabatic. Conversely, as the dynamic electron mass increases, the non-adiabatic effects become more prevalent. In this work, we are interested in varying  $M_e$  as a way to study the sensitivity of ion dynamics to non-adiabatic effects.

The eFF MD simulations in this work utilize the eFF implementation in the LAMMPS code [27]. The eFF simulations contained 1024 ions of H and 1024 electrons and were implemented in the microcanonical (NVE) ensemble. The simulation time step was  $1.0\times10^{-4}$  fs for  $M_e\geq1$   $m_e$ , where  $m_e$  is the physical electron mass, and the system was allowed to evolve for 2 ps after an equilibration time of 500 fs using a velocity rescaling thermostat. For  $M_e<1m_e$  the time step ranged from  $2.0\times10^{-6}-8.0\times10^{-5}$  fs, depending on temperature and density of the system. To prevent the electron wave packet from becoming excessively diffuse, the width was regulated using a restraining harmonic potential [9,28]. Due to the increased computational cost of eFF simulations with the small time step, we performed the  $M_e<1$   $m_e$  eFF simulations for 300 fs after equilibrating for 100 fs. In all cases, convergence with respect to total simulation time was

checked by evaluating the velocity auto-correlation function (VACF) sum rule,  $\langle \vec{v}(t=0) \cdot \vec{v}(0) \rangle = 3k_BT/m$ . We ensured the ions had reached equilibrium by verifying that the ion temperature did not fluctuate more than  $\pm 3\%$ , with no noticeable long-term drift. The electrons were verified to be in thermodynamic equilibrium with the ions based on the electron kinetic energy, which oscillated less than  $\pm 5\%$  during the simulation.

In order to directly connect the eFF results with the BO approximation, we require an equalfidelity adiabatic simulation method. We accomplish this using classical MD with a force-matched ion-ion potential. From Potfit, we extract an effective ion-ion potential defined by tabulated values and spline interpolation. Potfit implements the simulated annealing method to minimize the mean square deviations between a set of reference and calculated forces [29]. For this work, we use data from the eFF simulations as the reference forces in the force-matching algorithm. For each eFF simulation (i.e., at each specific temperature, density, and dynamic electron mass) we extract the forces from 32 reference configurations, uniformly selected from the simulation. In each case, we used a Yukawa potential with a Thomas-Fermi screening length as an initial guess for the force-matched potential. The effective potential obtained from Potfit contains the ensemble-averaged screening effects due to the presence of electrons in the eFF simulation. Potfit produces a forced-matched potential in an output file that can be read directly into LAMMPS to implement a classical MD simulation [30]. To ensure equality in underlying approximations and allow for a direct comparison between the adiabatic simulation (classical MD with force-matched potential) and the non-adiabatic simulation (eFF), we compare the radial distribution functions (RDF) at a given temperature and density. Furthermore, we include the RDF from the DFT-MD simulation in Fig. 1 (b) to provide more evidence for why eFF and DFT should not be compared. Each classical MD simulation had the same parameters as the corresponding eFF simulation; that is to say, the parameters were matched to the eFF simulations used to produce the force-matched potentials.

## 3. Results and Discussion

In Fig. 1 (a), we show an example force-matched potential generated from the eFF simulation with  $M_e=1~m_e$  for  $\rho=0.7~g/cm^3$  at T=4.5~eV. This potential is compared to a Coulomb potential and a Yukawa potential with an inverse screening length,  $\kappa$ , obtained by fitting the force-matched potential.  $\kappa$  is dimensionless with respect to the Wigner–Seitz radius, a, where  $a=(3/4)^{1/3}(\pi n)^{-1/3}$  and n is the ion particle density. The fitted Yukawa potential matches well with the force-matched potential, demonstrating that the potential obtained from eFF contains screening effects due to the electron-ion interactions, in agreement with previous work where the ion-ion interaction for warm dense hydrogen was shown to be Yukawa-like [31].

We compare the RDFs from the classical simulations to those produced from the eFF simulations to ensure the two methods describe the same thermodynamic state. Previous work has shown that non-adiabatic effects have little influence on the static structure factor [7]. Thus, the RDF, which is related to the static structure factor through a spatial Fourier transform, is also not expected to be impacted by non-adiabatic effects. We confirm this in Fig. 1 (b), which shows RDFs from simulations performed at the same thermodynamic conditions as in Fig. 1 (a). As expected, the RDFs from the eFF simulations using a dynamic electron mass of  $\rm M_e=1~m_e$  and  $\rm M_e=1836~m_e$  match.

In Fig. 1 (b), we demonstrate the validity of the force-matching algorithm by obtaining an effective ion-ion potential that reproduces the RDF of the non-adiabatic simulation. For the  $M_{\rm e}=1~{\rm m_e}$  case, we confirmed that the RDFs for eFF and classical simulations match. These results demonstrate that we have successfully obtained an effective ion-ion potential that captures the time and spatially averaged ion-ion interactions of the eFF simulation with the same level of underlying approximations. Furthermore, we find the same agreement for the  $M_{\rm e}=1836~{\rm m_e}$  case, which exhibits exaggerated non-adiabatic interactions. As the RDFs are required to match for our method to be legitimate, we perform this verification for all thermodynamic conditions investigated in this work (see supplemental material). We find that all RDFs, a static property

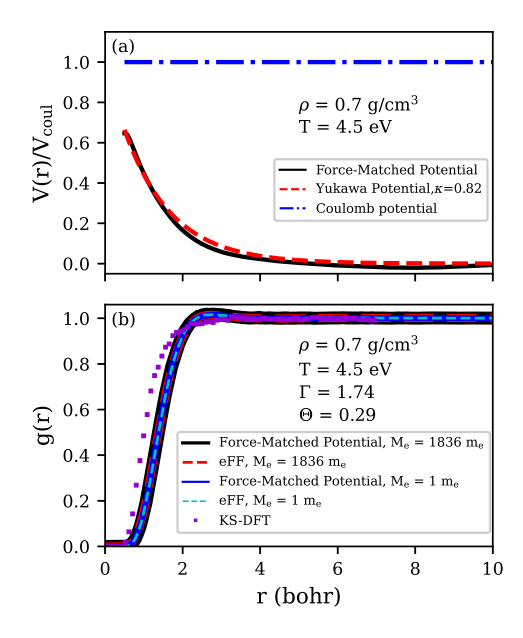


Figure 1. (a) Plot of ion-ion potential energy for a H plasma derived from an eFF simulation at  $\rho$  = 0.07 g/cm³, T = 4.5 eV, and  $M_e$  = 1  $m_e$ . The solid black line is the force-matched potential obtained from Potfit. The dashed red line is a Yukawa potential with an inverse screening length,  $\kappa$ , obtained by fitting to the force-matched potential.  $\kappa$  is dimensionless with respect to the Wigner–Seitz radius, a. The dot-dashed blue line is the Coulomb potential for reference. (b) Radial distribution functions (RDF) for warm dense hydrogen at the same thermodynamic conditions as figure (a). The solid black line represents the force-matched potential from Potfit generated from th eFF simulation with  $M_e$  = 1836  $m_e$ , the dashed red line represents the eFF simulation with  $M_e$  = 1836  $m_e$ , solid blue line represents the eFF simulation with  $M_e$  = 1  $m_e$ , the dashed light blue line represents the eFF simulation with  $M_e$  = 1  $m_e$ , and the purple squares represent the RDF from the KS-DFT simulation.

of the system, match regardless of how the non-adiabatic effects are scaled by modifying the dynamic electron mass in the corresponding eFF simulation.

We now focus on dynamic properties, where the importance of non-adiabatic effects is an open question. The Green-Kubo relation,

$$D = \frac{1}{3} \int_0^\infty \langle \vec{v}(0) \cdot \vec{v}(t) \rangle dt, \tag{3.1}$$

was used to calculate the ion self-diffusion coefficient, D, from both simulations using the VACF,  $\langle \vec{v}(0) \cdot \vec{v}(t) \rangle$  [32,33]. The calculated ion self-diffusion coefficient results for both simulation methods are given in Fig. 2 for several temperatures and densities spanning the WDM parameter space. The ion self-diffusion coefficient is plotted against the dynamic electron mass, which modifies the importance of non-adiabatic effects. The estimated uncertainty for the ion-self diffusion coefficients was less than 4% for all results (less than 2% for  $M_e \geq 1~m_e$ ) in Fig. 2. The details of the analysis methods used to obtain the ion self-diffusion coefficient and the uncertainty are outlined in the supplemental material.

In eFF, the ions experience the instantaneous force from electrons, whereas the force-matched potential only has the time-averaged effect of electrons. The classical MD generates an ion self-diffusion coefficient that is essentially independent of  $M_{\rm e}$  because the dependence on the dynamic electron mass is located in the kinetic energy component of the Hamiltonian [19], and for static, equilibrium properties, the partition function disassociates the kinetic energy and

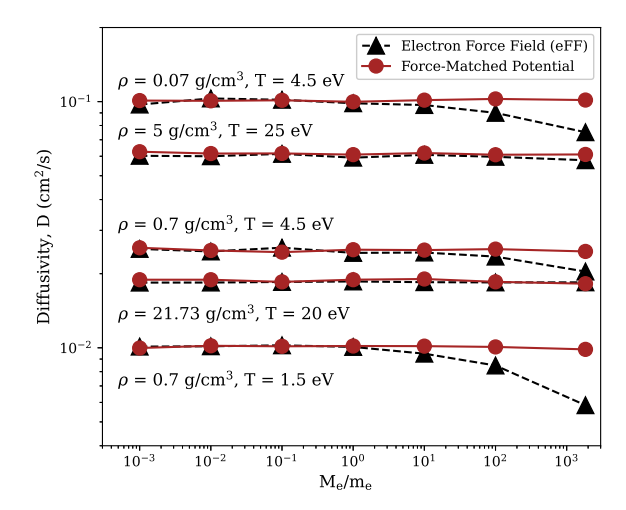


Figure 2. Ion self-diffusion coefficients obtained for a range of dynamic electron masses at various densities and temperatures from non-adiabatic and adiabatic simulations. The black line with triangles is the ion self-diffusion obtained from eFF simulations, and the brown line with circles is the ion self-diffusion obtained from classical MD simulations with the force-matched potential. The error bars were less than 4 % for all points (less than 2% for  $\rm M_e \geq 1~m_e)$  in the figure, and the error bars were smaller than the markers on the scale of the figure.

potential energy terms. Therefore, the configurational snapshots from the eFF simulations are static, equilibrium configurations of particles that will not include a significant mass dependence. The lack of mass dependence also explains why the RDF, a static equilibrium property, is equivalent for the classical MD and eFF simulations, but the self-diffusion coefficient, a dynamic property, is not. It should be noted that a different potential was obtained from the corresponding eFF simulation for each value of the dynamic electron mass, confirming that the force-matched potential is insensitive to non-adiabatic electron-ion interactions. Conversely, the ion self-diffusion coefficient obtained from the eFF simulations changes as the electron mass increases, demonstrating the effects of non-adiabatic electron-ion interactions on the ion self-diffusion coefficient

Differences in the ion self-diffusion coefficient between the two simulation techniques can be directly attributed to non-adiabatic effects. What can be seen in Fig. 2 is from  $\rm M_e=0.001~m_e$  to  $\rm M_e=1~m_e$ , the adiabatic and non-adiabatic simulation methods agree. That is, the ions only respond to the electron motion if  $\rm M_e$  is sufficiently large. Importantly, the two methods converge as the dynamic electron mass approaches zero, confirming that the eFF and classical simulations produce the same adiabatic limit. This is a critical difference from past efforts which compare eFF to DFT-MD [10], which do not agree in the adiabatic limit (c.f. Table 1) and therefore cannot be used to assess the importance of non-adiabatic effects.

For all temperatures and densities investigated, we find little difference between the two simulations at a dynamic electron mass of  $M_{\rm e}=1~\rm m_e$ , suggesting that non-adiabatic effects play little role in the WDM regime. However, we must take care with this interpretation as a varying dynamic electron mass has been used previously in eFF simulations to match experimental data [23,26]. Regardless, the ion self-diffusion coefficient is insensitive to the dynamic electron mass for the highest temperatures and densities investigated. Thus, its exact value is unimportant, suggesting that non-adiabatic effects are genuinely insignificant in this regime. However, at lower temperatures and densities, the ion self-diffusion coefficient exhibits greater sensitivity to the dynamic electron mass and its value must be calibrated using experimental data [34].

For the  $\rho$  = 0.07 g/cm<sup>3</sup> case, we see large sensitivity to the dynamic electron mass, but we do not know which value of M<sub>e</sub> is applicable to the WDM regime. Fortunately, a recent experiment

examined the ion-electron equilibration rate in liquid hydrogen at this density [35]. The ionelectron equilibration rate strongly depends on non-adiabatic effects, making it the ideal quantity to help set the dynamic electron mass in eFF simulations. To confirm the correct dynamic electron mass, we preformed three eFF simulations of electron-ion equilibration for different values of the dynamic electron mass, Me. In the simulations, two separate thermostats hold the electron and ion temperatures at 10 eV and 1 eV, respectively, to match the initial conditions of the experiment. Once the electrons and ions reached their respective temperatures, the thermostats disengaged, allowing them to equilibrate.

To extract the relaxation rates correctly, we implemented a two-temperature model [15] defined as follows:

$$c_i^0 \frac{dT_i}{dt} = g(T_e - T_i),$$

$$c_e \frac{dT_e}{dt} = g(T_i - T_e),$$
(3.2)

$$c_e \frac{dT_e}{dt} = g(T_i - T_e), (3.3)$$

where  $T_i$  is the ion temperature,  $T_e$  is the electron temperature,  $c_i^0 = \frac{3}{2}n_ik_B$  is the kinetic component of the heat capacity of the ions,  $n_i$  is the ion number density,  $c_e$  is the electronic heat capacity, and g is the electron-ion coupling factor. The coupled differential equations were solved iteratively to fit Eq. (3.2) and Eq. (3.3) to the electron and ion temperature data generated by eFF, where  $c_e$  and g were treated as constant fitting parameters. These two parameters were fit over multiple sub-intervals of the simulation data, with  $c_e$  and g found to remain constant to within 6% and 17%, respectively, over the temperature range of interest.

However, the electron heat capacity for eFF is known to be inaccurate, leading to the final equilibrium temperature in the eFF simulations being higher than the experimental data. This effect is attributed to the inclusion of the width of the single Gaussian electron wave packet, which acts as an additional degree of freedom in the dynamical equations of motion [28,36]. The electron heat capacity in all eFF simulations was found to be approximately  $2n_ek_B$  for all three dynamic electron masses, consistent with this description. To correct for this, the electron-ion equilibration curves shown in Fig. 3 are solutions to Eq. (3.2) and Eq. (3.3) utilizing the electron heat capacity inferred from the experimental data [35] while using the electron-ion coupling factor found from the eFF simulations. The corrected electron heat capacity is  $n_e k_B$ . In Fig. 3, we display the average result for an initial electron temperature of 10 eV, and we include the uncertainty due to the variation in the electron-ion coupling factor, g, with transparent bands.

Table 2 contains the values of  $\tau$  and g for all three values of  $M_e$  and  $\tau$  for two experimental results [35,37]. We also included the dynamic electron mass values of  $M_e = 2m_e$  and  $M_e = 3m_e$ to show the boundary of acceptable values. The errors in Table 2 include uncertainty arising from the experimental initial electron temperature, in addition to the variation of g from the eFF simulations, shown in Fig. 3. The equilibration time,  $\tau$ , is determined with  $c_e$ ,  $c_i^0$ , and g through the equation  $\tau = (c_e c_i^0)(c_e + c_i^0)^{-1}g^{-1}$ . Only the relaxation time obtained from simulations with  $\rm M_{\rm e}$  < 3  $\rm m_{\rm e}$  lie within the uncertainty of both experimental results.

Recall from Fig. 2 that for  $\rho = 0.07 \text{ g/cm}^3$  for values of  $M_e > 1 \text{ m}_e$  there were changes in the ion self-diffusion due to non-adiabatic effects. However, there was no way to establish the correct choice of  $M_e$  as past work has used various values of  $M_e$  [6,19,23,26]. We now have independent support for choosing  $M_e = 1 m_e$ , and we conclude non-adiabatic effects do not substantively affect the ion self-diffusion.

#### 4. Conclusion

In this work, we have developed a new method that disentangles non-adiabatic from adiabatic electron-ion interactions in MD simulations, independent of underlying model approximations. We demonstrated that the RDF, much like the static structure factor, is insensitive to non-adiabatic effects. We have used this to compare the ion self-diffusion coefficient from the non-adiabatic eFF computational model to an adiabatic, classical MD simulation. The method conclusively shows

**Table 2.** Electron-ion relaxation time from eFF and experiments for hydrogen at  $\rho=0.07$  g/cm $^3$ . The uncertainty for the eFF simulations takes into account the large error in the initial electron temperature from the experimental data and the uncertainty in g obtained from the eFF simulations.

	$g/10^{17}  (\mathrm{Wm^{-3}K^{-1}})$	$\tau$ (ps)
$eFF M_e = 1 m_e$	$5.66^{+0.82}_{-1.84}$	$0.62^{+0.29}_{-0.08}$
$eFF\ M_e = 2\ m_e$	$7.51_{-1.94}^{+2.35}$	$0.47^{+0.16}_{-0.11}$
$eFF M_e = 3 m_e$	$8.88^{+2.42}_{-2.42}$	$0.39^{+0.15}_{-0.08}$
$eFF M_e = 10 m_e$	$16.27^{+5.39}_{-5.29}$	$0.21^{+0.11}_{-0.05}$
$eFF\ M_e = 100\ m_e$	$36.94^{+13.59}_{-16.87}$	$0.09^{+0.08}_{-0.03}$
Fletcher et. al. [35]		$1.22_{-0.77}^{+0.77}$
Zastrau et. al. [37]		$0.90^{+0.30}_{-0.30}$

that at the highest temperature and density values investigated, ion self-diffusion is insensitive to non-adiabatic effects. At lower temperatures and densities, we show how the dynamic electron mass, which must be set empirically, increased the influence of non-adiabatic effects. In this regime, we set the dynamic electron mass using experimental temperature equilibration data in warm dense hydrogen, noting that non-adiabatic effects play a crucial role in temperature equilibration. Ultimately, we find  $M_{\rm e} < 3~m_{\rm e}$  fits both experimental electron-ion relaxation times confirming that non-adiabatic effects also have a negligible influence on the ion self-diffusion coefficient at lower temperatures and densities. Our results show that great care must be taken when comparing the difference between adiabatic and non-adiabatic techniques with varying levels of approximations and ultimately validate the Born-Oppenheimer approximation in calculations of the ion transport coefficients across the WDM regime.

Funding. This work was supported by the National Science Foundation under Grant No. PHY-2045718. This work was funded in part by the US Department of Energy, National Nuclear Security Administration (NNSA)

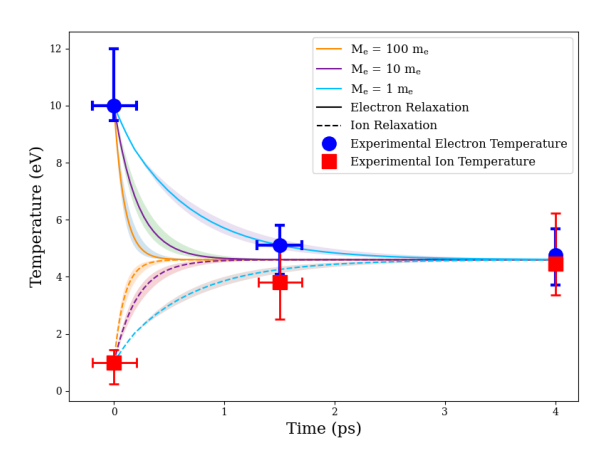


Figure 3. Electron-ion temperature relaxation versus time for the corrected eFF heat capacity, as described in the main text. The solid lines represent the electron temperature, and the dashed lines represent the corresponding hydrogen ion temperature. The orange color represents  $M_{\rm e}$  = 100  $m_{\rm e}$ , the purple color represents  $M_{\rm e}$  = 10  $m_{\rm e}$ , and the light blue color represents  $M_{\rm e}$  = 1  $m_{\rm e}$ , where  $m_{\rm e}$  is the physical mass of the electron. The blue circles are the experimentally measured electron temperatures, and the red squares are the corresponding experimental ion temperatures [35]. The bands around the lines represent the uncertainty due to the uncertainty in the electron-ion coupling factor, g, obtained from the eFF simulation.

(Award No. DE-NA0004039). N.R.S. acknowledges support by the Department of Energy NNSA under Award Number DE-NA0003856, and the New York State Energy Research and Development Authority. This report was prepared as an account of work sponsored by an agency of the U.S. Government. Neither the U.S. Government nor any agency thereof, nor any of their employees, makes any warranty, express or implied, or assumes any legal liability or responsibility for the accuracy, completeness, or usefulness of any information, apparatus, product, or process disclosed, or represents that its use would not infringe privately owned rights. Reference herein to any specific commercial product, process, or service by trade name, trademark, manufacturer, or otherwise does not necessarily constitute or imply its endorsement, recommendation, or favoring by the U.S. Government or any agency thereof. The views and opinions of authors expressed herein do not necessarily state or reflect those of the U.S. Government or any agency thereof.

# References

- 1. Ichimaru S. 1982 Strongly coupled plasmas: high-density classical plasmas and degenerate electron liquids. *Rev. Mod. Phys.* **54**, 1017–1059. Publisher: American Physical Society (10.1103/RevModPhys.54.1017)
- 2. Lorenzen W, Becker A, Redmer R. 2014 Progress in Warm Dense Matter and Planetary Physics. In Graziani F, Desjarlais MP, Redmer R, Trickey SB, editors, *Frontiers and Challenges in Warm Dense Matter*, Lecture Notes in Computational Science and Engineering pp. 203–234. Cham: Springer International Publishing.
- 3. Tully JC. 1990 Molecular dynamics with electronic transitions. *J. Chem. Phys.* **93**, 1061–1071. (10.1063/1.459170)
- 4. Martin RM. 2020 *Electronic Structure: Basic Theory and Practical Methods*. Cambridge, United Kingdom; New York, NY: Cambridge University Press 2nd edition edition.
- 5. Cramer CJ. 2004 Essentials of Computational Chemistry: Theories and Models. Chichester, West Sussex, England; Hoboken, NJ: Wiley 2nd edition edition.
- Su JT, Goddard WA. 2007 Excited Electron Dynamics Modeling of Warm Dense Matter. Phys. Rev. Lett. 99, 185003. (10.1103/PhysRevLett.99.185003)
- 7. Mabey P, Richardson S, White TG, Fletcher LB, Glenzer SH, Hartley NJ, Vorberger J, Gericke DO, Gregori G. 2017 A strong diffusive ion mode in dense ionized matter predicted by Langevin dynamics. *Nature Communications* 8, 14125. Number: 1 Publisher: Nature Publishing Group (10.1038/ncomms14125)
- 8. Larder B, Gericke DO, Richardson S, Mabey P, White TG, Gregori G. 2019 Fast nonadiabatic dynamics of many-body quantum systems. *Science Advances* 5, eaaw1634. Publisher: American Association for the Advancement of Science Section: Research Article (10.1126/sciadv.aaw1634)
- 9. Davis RA, Angermeier WA, Hermsmeier RKT, White TG. 2020 Ion modes in dense ionized plasmas through nonadiabatic molecular dynamics. *Phys. Rev. Research* **2**, 043139. Publisher: American Physical Society (10.1103/PhysRevResearch.2.043139)
- 10. Yao Y, Zeng Q, Chen K, Kang D, Hou Y, Ma Q, Dai J. 2021 Reduced ionic diffusion by the dynamic electron–ion collisions in warm dense hydrogen. *Physics of Plasmas* **28**, 012704. (10.1063/5.0028925)
- 11. Grabowski PE, Hansen SB, Murillo MS, Stanton LG, Graziani FR, Zylstra AB, Baalrud SD, Arnault P, Baczewski AD, Benedict LX, Blancard C, Čertík O, Clérouin J, Collins LA, Copeland S, Correa AA, Dai J, Daligault J, Desjarlais MP, Dharma-wardana MWC, Faussurier G, Haack J, Haxhimali T, Hayes-Sterbenz A, Hou Y, Hu SX, Jensen D, Jungman G, Kagan G, Kang D, Kress JD, Ma Q, Marciante M, Meyer E, Rudd RE, Saumon D, Shulenburger L, Singleton RL, Sjostrom T, Stanek LJ, Starrett CE, Ticknor C, Valaitis S, Venzke J, White A. 2020 Review of the first charged-particle transport coefficient comparison workshop. *High Energy Density Physics* 37, 100905. (10.1016/j.hedp.2020.100905)
- 12. Orekhov ND, Stegailov VV. 2016 Electron–ion relaxation in Al nanoplasma: Wave packet molecular dynamics. *J. Phys.: Conf. Ser.* 774, 012104. (10.1088/1742-6596/774/1/012104)
- 13. Ma Q, Dai J, Kang D, Murillo M, Hou Y, Zhao Z, Yuan J. 2019 Extremely Low Electronion Temperature Relaxation Rates in Warm Dense Hydrogen: Interplay between Quantum Electrons and Coupled Ions. *Phys. Rev. Lett.* **122**, 015001. (10.1103/PhysRevLett.122.015001)
- 14. Salzmann D. 1998 *Atomic physics in hot plasmas*. International series of monographs on physics ; 97. New York: Oxford University Press. Publication Title: Atomic physics in hot plasmas.

- 15. Daligault J, Simoni J. 2019 Theory of the electron-ion temperature relaxation rate spanning the hot solid metals and plasma phases. *Phys. Rev. E* **100**, 043201. Publisher: American Physical Society (10.1103/PhysRevE.100.043201)
- 16. Klakow D, Toepffer C. 1994 Hydrogen under extreme conditions. *Phys. Lett. A.* **192**, 55–59. (10.1016/0375-9601(94)91015-4)
- 17. Morozov IV, Valuev IA. 2009 Localization constraints in Gaussian wave packet molecular dynamics of nonideal plasmas. *J. Phys. A: Math. Theor.* **42**, 214044. (10.1088/1751-8113/42/21/214044)
- 18. Angermeier WA, White TG. 2021 An Investigation into the Approximations Used in Wave Packet Molecular Dynamics for the Study of Warm Dense Matter. *Plasma* 4, 294–308. (10.3390/plasma4020020)
- 19. Su JT, Goddard WA. 2009 The dynamics of highly excited electronic systems: Applications of the electron force field. *J. Chem. Phys.* **131**, 244501. (10.1063/1.3272671)
- 20. Brommer P, Gähler F. 2006 Effective potentials for quasicrystals from ab-initio data. *Philosophical Magazine* **86**, 753–758. (10.1080/14786430500333349)
- 21. Brommer P, Gähler F. 2007 Potfit: effective potentials fromab initiodata. *Modelling Simul. Mater. Sci. Eng.* **15**, 295–304. (10.1088/0965-0393/15/3/008)
- 22. Brommer P, Kiselev A, Schopf D, Beck P, Roth J, Trebin HR. 2015 Classical interaction potentials for diverse materials fromab initiodata: a review ofpotfit. *Modelling Simul. Mater. Sci. Eng.* 23, 074002. (10.1088/0965-0393/23/7/074002)
- 23. Su JT, Goddard WA. 2009 Mechanisms of Auger-induced chemistry derived from wave packet dynamics. *Proceedings of the National Academy of Sciences* **106**, 1001–1005. (10.1073/pnas.0812087106)
- 24. Kim H, Su JT, Goddard WA. 2011 High-temperature high-pressure phases of lithium from electron force field (eFF) quantum electron dynamics simulations. *Proceedings of the National Academy of Sciences* **108**, 15101–15105. (10.1073/pnas.1110322108)
- 25. Theofanis PL, Jaramillo-Botero A, Goddard WA, Mattsson TR, Thompson AP. 2012a Electron dynamics of shocked polyethylene crystal. *Phys. Rev. B* **85**, 094109. (10.1103/PhysRevB.85.094109)
- 26. Theofanis PL, Jaramillo-Botero A, Goddard WA, Xiao H. 2012b Nonadiabatic Study of Dynamic Electronic Effects during Brittle Fracture of Silicon. *Phys. Rev. Lett.* **108**, 045501. (10.1103/PhysRevLett.108.045501)
- 27. Jaramillo-Botero A, Su J, Qi A, Goddard WA. 2011 Large-scale, long-term nonadiabatic electron molecular dynamics for describing material properties and phenomena in extreme environments. *Journal of Computational Chemistry* **32**, 497–512. (https://doi.org/10.1002/jcc.21637)
- 28. Grabowski PE. 2014 A Review of Wave Packet Molecular Dynamics. In Graziani F, Desjarlais MP, Redmer R, Trickey SB, editors, *Frontiers and Challenges in Warm Dense Matter*, Lecture Notes in Computational Science and Engineering pp. 265–282. Cham: Springer International Publishing.
- 29. Brommer P. 2008 Development and test of interaction potentials for complex metallic alloys. phd University of Stuttgart. (10.18419/opus-4819)
- 30. Thompson AP, Aktulga HM, Berger R, Bolintineanu DS, Brown WM, Crozier PS, in 't Veld PJ, Kohlmeyer A, Moore SG, Nguyen TD, Shan R, Stevens MJ, Tranchida J, Trott C, Plimpton SJ. 2022 LAMMPS a flexible simulation tool for particle-based materials modeling at the atomic, meso, and continuum scales. *Computer Physics Communications* **271**, 108171. (10.1016/j.cpc.2021.108171)
- 31. Vorberger J, Gericke DO. 2013 Effective ion–ion potentials in warm dense matter. *High Energy Density Physics* **9**, 178–186. (10.1016/j.hedp.2012.12.009)
- 32. Evans DJ, Morriss GP. 2008 Statistical Mechanics of Nonequilibrium Liquids vol. 2nd ed. Cambridge: Cambridge University Press.
- 33. Hansen JP, McDonald IR. 2013 *Theory of Simple Liquids: With Applications to Soft Matter*. San Diego, CA: Elsevier Science & Technology 4 edition.
- 34. Grabowski PE, Markmann A, Morozov IV, Valuev IA, Fichtl CA, Richards DF, Batista VS, Graziani FR, Murillo MS. 2013 Wave packet spreading and localization in electron-nuclear scattering. *Phys. Rev. E* 87, 063104. (10.1103/PhysRevE.87.063104)
- 35. Fletcher LB, Vorberger J, Schumaker W, Ruyer C, Goede S, Galtier E, Zastrau U, Alves EP, Baalrud SD, Baggott RA, Barbrel B, Chen Z, Döppner T, Gauthier M, Granados E, Kim JB,

- Kraus D, Lee HJ, MacDonald MJ, Mishra R, Pelka A, Ravasio A, Roedel C, Fry AR, Redmer R, Fiuza F, Gericke DO, Glenzer SH. 2022 Electron-Ion Temperature Relaxation in Warm Dense Hydrogen Observed With Picosecond Resolved X-Ray Scattering. *Frontiers in Physics* 10. (10.3389/fphy.2022.838524)
- 36. Su JT. 2007 An Electron Force Field for Simulating Large Scale Excited Electron Dynamics. phd California Institute of Technology.
- 37. Zastrau U, Sperling P, Harmand M, Becker A, Bornath T, Bredow R, Dziarzhytski S, Fennel T, Fletcher L, Förster E, Göde S, Gregori G, Hilbert V, Hochhaus D, Holst B, Laarmann T, Lee H, Ma T, Mithen J, Mitzner R, Murphy C, Nakatsutsumi M, Neumayer P, Przystawik A, Roling S, Schulz M, Siemer B, Skruszewicz S, Tiggesbäumker J, Toleikis S, Tschentscher T, White T, Wöstmann M, Zacharias H, Döppner T, Glenzer S, Redmer R. 2014 Resolving Ultrafast Heating of Dense Cryogenic Hydrogen. *Phys. Rev. Lett.* 112, 105002. (10.1103/PhysRevLett.112.105002)